

---

# Phonon scatterings in the lattice thermal conductivity of $\text{Si}_{1-x}\text{Ge}_x$ alloy nanowires: Theoretical study

Soran Mohammed Mamand

Department of Physics, Faculty of Science and Science Education, University of Sulaimani, Sulaimanyah, Iraqi Kurdistan, Iraq

**Email address:**

soran.mamand@univsul.net

**To cite this article:**

Soran Mohammed Mamand. Phonon Scatterings in the Lattice Thermal Conductivity of  $\text{Si}_{1-x}\text{Ge}_x$  Alloy Nanowires: Theoretical Study. *American Journal of Nanoscience and Nanotechnology*. Vol. 2, No. 2, 2014, pp. 21-27. doi: 10.11648/j.nano.20140202.12

---

**Abstract:** Theoretical investigation of the alloy concentration and temperature dependences of the lattice thermal conductivity of silicon-germanium nanowires is performed using the Steigmeier and Abeles model. Phonon scattering processes are represented by frequency-dependent relaxation time approximation. In addition to the commonly considered acoustic three-phonon umklapp processes, phonon-boundary and point-defect scattering mechanisms are assumed. No distinction is made between longitudinal and transverse phonons. The importance of all the mechanisms involved in the model is clearly demonstrated. Analysis of the results shows that: (1) alloy scattering is the dominant scattering mechanism at intermediate and high temperatures; (2) thermal conductivity is mainly depends on the alloy concentration across the full range of temperatures; (3) weak diameter dependence of thermal conductivity is observed in  $\text{Si}_{1-x}\text{Ge}_x$  alloy nanowires; (4) the roughness of nanowires depends on the alloy concentration and has a major role in decreasing thermal conductivity at low temperatures; (5) the anharmonicity parameter is not size-dependent, as compared to Si and Ge nanowires. These findings provide new insights into the fundamental understanding of high-performance nanostructural semiconductors of relevance to optoelectronic and thermoelectric devices.

**Keywords:** SiGe Alloy, Lattice Thermal Conductivity, Phonon Scattering, Nanowires

---

## 1. Introduction

The advances in nanomaterials modeling coupled with new characterization tools are the key to studying new properties and capabilities and then to designing devices with improved performance [1-3]. Direct energy conversion between heat and electricity based on the thermoelectric effect is attractive for its potential applications in the area of waste heat recovery and environmentally friendly refrigeration [4]. The thermoelectric figure of merit (ZT), an indicator of conversion efficiency, which is proportional to the electrical conductivity,  $\sigma$ , the square of the Seebeck coefficient,  $S$ , and the absolute temperature,  $T$ , and inversely proportional to the thermal conductivity (TC), correlate strongly, making ZT improvement difficult [5,6]. A device made from a material with a high ZT value should have high conversion efficiency. A key feature of nanostructured semiconductor materials is the reduction in TC by scattering phonons with mean free paths larger than the characteristic dimensions of the nanostructured material while maintaining the electronic properties [7]. Thus,

theoretical prediction of the TC of nanostructure materials prior to their fabrication is a desirable goal, both from the applied and basic research points of view.

In the past decade, much research has reported increased ZT, mainly from TC reduction due to nanostructuring [7-9]. The search for new approaches to facilitate highly efficient thermoelectrics is far from over, especially with the introduction of low-dimensional structures such as nanowires (NWs); the reduced TC reported for NWs is due not only to boundary scattering, but also includes a surface roughness component [10-12]. It has been shown that single Si NWs exhibit 60 times higher ZT than Si bulk [13]. The use of nanostructures to boost ZT and the introduction of alloys can further reduce TC via alloy scattering without deterioration in other performance parameters [7]. Since silicon-germanium ( $\text{Si}_{1-x}\text{Ge}_x$ , where  $x$  is the molar fraction of Ge) alloys have, to date, been the only proven thermoelectric materials in power generation devices operating across a large temperature range for heat conversion into electricity using a radioisotope heat source [4,14], many efforts have been made to enhance the ZT of

$\text{Si}_{1-x}\text{Ge}_x$  bulk alloys [15-19]. Recently, many researchers [20-23] have experimentally synthesized  $\text{Si}_{1-x}\text{Ge}_x$  NWs with different diameters and Ge concentrations. They have measured the TC of these NWs and shown that these NWs have TC values lower than that of their bulk value; they have attributed this decrease in TC to the dominance of alloy and boundary scattering mechanisms in  $\text{Si}_{1-x}\text{Ge}_x$  NWs. These latter experimental measurements deserve theoretical study in order to clarify scattering mechanisms across the full temperature range and elucidate the role of parameters and diameter dependency in  $\text{Si}_{1-x}\text{Ge}_x$  alloy NWs, which is the goal of the present work.

## 2. Theory

Thermal conduction in semiconductors relies mostly on acoustic phonons [24]. Their contribution to the TC of a system is due to various phonon scattering mechanisms and substantially depends on the temperature, as this determines which phonons contribute most, as well as on the phonon spectrum. However, when acoustically mismatched barriers are present in materials, spatial confinement of phonon occurs, resulting in modification to and quantization of the phonon spectrum [25], consequently, phonon group velocity will decrease compared to that in the bulk. This can lead to considerable reductions in TC [26].

In general, TC ( $k$ ) is a tensor, for an isotropic solid it is a scalar. There are generally two contributions, namely electronic TC ( $k_e$ ) and lattice or phonon TC ( $k_l$ ):  $k = k_e + k_l$ . None of the NW samples treated in this work are intentionally doped, they are relatively defect free and pure [21-23], so the electronic contribution is neglected and only the lattice contribution is taking into account. Steigmeier and Abeles' model [27] of the lattice thermal conductivity (LTC) of bulk alloys, based on the Callaway's model [28], was used in this work. Their model treats phonons with the Boltzmann transport equation under a relaxation time approximation. In this model, the contribution of optical modes to thermal resistivity is neglected [27,29]. Thus this model is given by:

$$k_l = 4.67 \times 10^{-2} \left( \frac{\theta^2}{\delta} \right) (I_1 + I_2^2 / I_3) \quad (1)$$

where:

$$I_1 = \int_0^1 \alpha w_N^2 \left( (w_N \theta / T)^2 e^{w_N \theta / T} / (e^{w_N \theta / T} - 1)^2 \right) dw_N,$$

$$I_2 = 2 \int_0^1 (\tau / \tau_U) w_N^2 \left( (w_N \theta / T)^2 e^{w_N \theta / T} / (e^{w_N \theta / T} - 1)^2 \right) dw_N,$$

$$I_3 = 2 \int_0^1 (1 / \tau_U) (1 - (2\tau / \tau_U)) w_N^2 \left( (w_N \theta / T)^2 e^{w_N \theta / T} / (e^{w_N \theta / T} - 1)^2 \right) dw_N,$$

Here:  $w_N = \hbar w / k_B \theta$  is the normalized phonon frequency,  $w$  is the phonon frequency,  $\theta$  is the Debye

temperature,  $k_B$  and  $\hbar$  are the Boltzmann and Planck constants, respectively.  $\tau$  is the combined (total) phonon relaxation time,  $\tau_U$  is the relaxation time due to umklapp scattering, and  $\delta$  is the cubed root of the atomic volume ( $V$ ).

Phonon scattering processes can be divided into intrinsic processes arising from the anharmonicity of interatomic forces and extrinsic processes due to phonons scattering at the boundaries of the crystal and at the sites of various sorts of crystal defects and imperfections (e.g. point defects, impurities, dislocations, alloy disorders, embedded nanoparticles etc.). Anharmonic three-phonon scattering processes are of two distinct types: normal scattering processes (N-processes) which conserve the total crystal momentum after a collision, and umklapp scattering processes (U-processes) for which the total crystal momentum changes by a reciprocal lattice vector after a collision [30]. On the other hand, not all extrinsic scattering processes conserve total crystal momentum after a collision. Each scattering process is described by a relaxation time which, naturally, is a function of the phonon wave vector [28]. It also depends on the nature of the scattering mechanism and the coefficients characteristic of this mechanism. Generally, relaxation times are expressed as functions of phonons' intrinsic frequency instead of as a wave vector [16,24,31]. Depending on the nature of the scattering mechanism, relaxation times have different forms of expression. Three different scattering mechanisms are assumed in the present study to describe the processes which a phonon can undergo in alloy NWs as follows:

i. Intrinsic U-processes: an analytical expression to describing U-processes is assumed, this has been derived via a physically reasonable experimental method and describes the U-processes in several high purity crystals [32]. In the alloying materials, the relaxation time due to N-processes is much greater than the total relaxation time, thus N-processes can be neglected [33]. The scattering rate due to U-processes is of the form [32]:

$$[\tau_U]^{-1} = A_U w^2 T \exp(-\theta / 3T) \quad (2)$$

where:  $A_U = \hbar \gamma^2 / M v^2 \theta$

Here:  $\gamma$ ,  $M$ , and  $v$  are the Gruneisen parameter, atomic mass, and phonon group velocity, respectively. The phonon group velocity for  $\text{Si}_{1-x}\text{Ge}_x$  alloy NWs can be found from [34]:

$$v^{-2} = (1-x) v_{\text{Si}}^{-2} + x v_{\text{Ge}}^{-2} \quad (3)$$

ii. Phonon-alloying scattering: the assumption is made that the lattice disorder due to alloying can be described by point-defect scattering [27]. The relaxation time ( $\tau_A$ ) for point-defect scattering due to lattice disorder in alloys is given by [24]:

$$[\tau_A]^{-1} = B_A w^4 \quad (4)$$

where :  $B_A = \delta^3 \Gamma / 4\pi v^3$

Here:  $\Gamma$  denotes the phonon-scattering parameter that takes into account the contributions from mass differences, atomic size differences and bond strength differences between the impurity (imperfection) and the host lattice atom. Since the semiconductor crystal is treated as an elastic isotropic continuum medium, no much additional errors will be introduced by neglecting the contribution of bond strength and considering only the mass-difference contribution. The alloy is assumed to be a random mixture of atoms with different masses and volumes arranged in a lattice. In this case of alloy disorder scattering,  $\Gamma$  represents the disorder parameter and is calculated using the virtual lattice approach given by [27, 35]:

$$\Gamma = x(1-x) \left[ (\Delta M / M)^2 + \varepsilon (\Delta \delta / \delta)^2 \right]$$

Where:

$$\begin{aligned} \Delta M &= M_{Si} - M_{Ge}, \\ \Delta \delta &= \delta_{Si} - \delta_{Ge}, \\ M &= (1-x)M_{Si} - xM_{Ge}, \\ \delta &= (1-x)\delta_{Si} - x\delta_{Ge}. \end{aligned}$$

Here:  $\varepsilon$  is a parameter of the order 40 [35]. After inserting numerical values for physical constants into Eq.(3), the phonon group velocity,  $v$ , is assumed to be given by the Debye expression,  $v = (k_B / \hbar) (6\pi^2)^{-1/3} \theta \delta$ ; and using the normalized frequency,  $w_N$ , the following expression results for the relaxation time,  $\tau_A$ , given by [27]:

$$\left[ \tau_A \right]^{-1} = 6.17 \times 10^{11} \times \Gamma \times \theta \times w_N^4 \quad (5)$$

iii. Phonon-boundary scattering: phonon-boundary scattering was first investigated by Casimir [36]. Later, Berman et al. [37] extended Casimir's theory to include the effects of the finite size and non-zero specularity parameter of phonons ( $P$ ). However, Zimann [38] and later Soffer [39], developed a statistical model for the reflection of a plane wave from a rough surface. It has been shown that the reflectivity of a plane wave from a rough surface leads to a plane wave in the specular direction and to a diffused plane wave in a direction that depends on the incident plane wave, the surface roughness and the tangential correlation of the surface asperities [38,39]. Assuming the partial specular reflection of phonons at sample surfaces, the phonon-boundary scattering rate is given by [40]:

$$\left[ \tau_B \right]^{-1} = v \left[ (1/L_C)(1-P/1+P) + (1/l) \right] \quad (6)$$

Where:  $L_C$  is the mean free path or characteristic length of a phonon,  $l$  is the length of the sample, and  $P$  is specularity parameter, which is used as the free adjustable parameter since there are no precise experimental data for the roughness values of the  $Si_{1-x}Ge_x$  alloy NW surfaces

investigated.

The inverse of the total resistive relaxation time ( $\tau$ ), accounting for all the phonon scattering processes that destroy the total crystal momentum, is given according to Mathiessen's rule:

$$\left[ \tau \right]^{-1} = \left[ \tau_B \right]^{-1} + \left[ \tau_U \right]^{-1} + \left[ \tau_A \right]^{-1} \quad (7)$$

### 3. Results and Discussion

Figure 1 displays the theoretical calculation results for the temperature variation in the LTC of  $Si_{1-x}Ge_x$  alloy NWs in the temperature range 20 to 400K using Eqs.(1-7). The diameters considered are 147, 344, 229 and 160nm, with Ge concentrations of 0.004, 0.04, 0.04 and 0.09, respectively. These particular values were chosen in order to compare with the experimental results reported by Kim et al. [21].  $L_C$  is limited by the sample diameter and  $l = 10$  micrometers [21]. The constant parameters used in the calculations are listed in Table 1. Using an adjustable parameter, which is usual in the literature [41-44], attempts were made to use the three parameters,  $\theta$ ,  $\gamma$  and  $P$ , as adjustable parameters to correlate the calculated LTC to that of the corresponding experimental data at [21]. The values of  $\theta$ ,  $\gamma$  and  $P$  were adjusted such that the best fit for calculated LTC to the experimental data was obtained. In the calculations, the electron-phonon scattering rate was assumed (tested) to be as in our previous work [44] and the results changed by less than 2%, accordingly, this scattering rate was neglected.

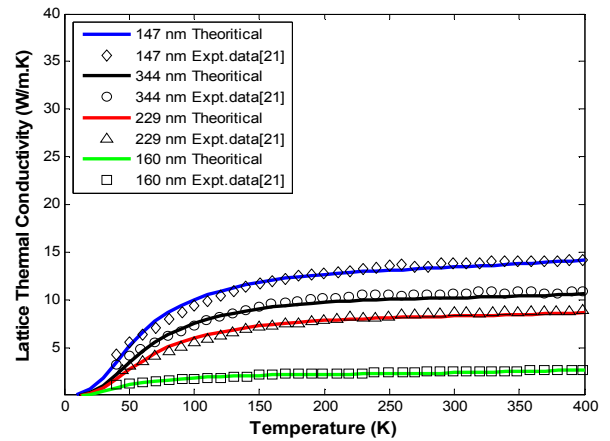


**Figure 1.** (Color online) Temperature variation of the LTC of four samples of  $Si_{1-x}Ge_x$  alloy NWs Experimental data are from [21]. Solid lines represent the present theoretical work.

The high surface-to-volume ratio of semiconductor NWs can dramatically alter their fundamental properties with respect to corresponding bulk samples [45]. Balandin and Wang [25] have demonstrated that acoustic-phonon dispersion relations in nanostructures can be modified from the bulk due to the phonon confinement effect. Phonon confinement (which reduces phonon group velocity), however, can lead to considerable reductions of LTC in

NWs [25,45]. For the aforementioned sample of  $\text{Si}_{1-x}\text{Ge}_x$  alloy NWs, phonon group velocities are assumed to be size-dependent (as a result of phonon confinement) and calculated using a thermodynamical approach, as used in previous work [44], with all the parameters of Si and Ge available at [46,47]. It is found that the decrease in the phonon group velocities is less than 5.5% of that of the bulk values of the samples, this is because of the relatively large diameter of the samples. The decrease in the phonon group velocity is significant for nanowires of diameter less than 100nm (called a small diameter in this work) [44-46]. So, the phonon group velocities of bulk Si and Ge (as shown in Table 1) were used (using Eq.(3)) to calculate the phonon group velocities of the sample of  $\text{Si}_{1-x}\text{Ge}_x$  alloy NWs.

**Table 1.** Geometrical properties of the bulk silicon and germanium crystals used in the calculation of LTC.

Material	M * 10 <sup>-26</sup> (Kg)	V * 10 <sup>-29</sup> (m <sup>3</sup> )	$\theta$ (K)	$\nu$ (m/sec)
Si	4.66 <sup>a</sup>	2 <sup>a</sup>	645 <sup>b</sup>	8430 <sup>b</sup>
Ge	12 <sup>a</sup>	2.25 <sup>a</sup>	374 <sup>b</sup>	4920 <sup>b</sup>

a: from [43], b: from [48].

The Debye temperature,  $\theta$ , is a key parameter that determines thermal transport dynamics properties, it is related to the cutoff frequency,  $w_c$ , by the relation  $\theta = \hbar w_c / k_B$  and depends on the true density of state properly weighted in the Brillouin zone [49]. The cutoff frequency is the only parameter that relies on nanowire measurements [34]. Following the procedure at [34,41] a very good description of NW thermal conductivity can be obtained without the need to compute the full dispersions by introducing an adjustable parameter, the cutoff frequency or the Debye temperature. So, the Debye temperature is taken into account as a free adjustable parameter with permitted values below the bulk value. However, the Debye temperature which is involved in the expression of the phonon scattering rates due to U-processes and alloying has a noticeable influence on LTC at intermediate and high temperatures. Thus, the Debye temperature values used to obtain the best fit to the experimental data are shown in Table 2.

**Table 2.** Fitting parameters of the  $\text{Si}_{1-x}\text{Ge}_x$  alloy NWs used to calculate the LTC of each NW. The samples are from [21].

Ge concentration	Diameter (nm)	$\theta$ (K)	$P$	$\gamma$
0.004	147	150	0.92	0.8
0.04	344	440	0.88	0.79
0.04	229	420	0.84	0.78
0.09	160	340	0.75	0.77

As shown in figure 1, the dramatic decrease in the LTC of  $\text{Si}_{1-x}\text{Ge}_x$  alloy NWs is due to alloy concentration. The NW of the lowest concentration (0.004) which has the lowest diameter (147 nm) has a higher LTC, this is due to the dominance of alloy effects relative to the other three

NWs. Meanwhile the two NWs of diameters 344 and 229 nm both have the same Ge concentration (0.04); the former has an LTC 7% higher than the latter at 300K, indicating that increasing the surface to volume ratio (or decreasing the diameter) will cause the surface effect to become more effective for NWs of the same alloy concentration. Description and elucidation across the full temperature range of the effect of phonon scattering rates and parameters is as follows:

A boundary effect controls phonon scattering at very low temperatures, and this depends on the surface quality and size [45,47,50]. Boundary scattering reduces phonons' mean free path and increases the thermal resistance (surface effect), while phonon confinement (size effect) leads to a flattening of phonon dispersion and decreases phonon group velocity [25,50]. The decrease in phonon group velocity causes an increase in the scatter rate, as well as a decrease in the boundary scatter rate. Therefore, the effects of boundary scattering and phonon confinement should be considered together when calculating LTC [51]. In alloy NWs, thermal conductivity is more sensitive to surface effect than size effect [21,22]. However, it is reported that the LTC of  $\text{Si}_{1-x}\text{Ge}_x$  alloy NWs of small diameter is proportional to nanowire diameter, whereas this dependence becomes less as the diameter increases [34]. This lower dependence is related to the very fast frequency dependence of alloy scattering. Alloy scattering blocks high frequency phonons very effectively, but it is totally transparent to low frequency phonons. Thus, the LTC of an alloy is dominated by low frequency phonons with very long mean free paths, whereas in non-alloys, the LTC has contributions from a larger range of frequencies with shorter mean free paths on average [34].

As the concentration of Ge increases, the specularity parameter,  $P$ , will decrease (see Table 2); consequently, roughness (root mean square height deviation of the surface) will increase [38], which causes an increase in the rate of diffuse boundary scattering, thereby thermal resistance will increase too [25]. A detailed explanation of this effect can be found in previous work of GaN NWs [44] and Si NWs [46]. But a difference between previous work and present work is that while the specularity parameter depends on the size of GaN and Si NWs, in  $\text{Si}_{1-x}\text{Ge}_x$  alloy NWs this depends on the alloy concentration, as shown in figure 2 (the role of parameters will be discussed later). This result is related to the phonon mean free path in various conditions, which suggests that dense surface features may enhance surface scattering, thereby hindering phonon transport and decreasing LTC [52]. Thus, size dependence is not as effective as alloy scattering, especially for relatively large diameters, and is not as significant as it is in the case of Si, Ge and GaN NWs [44,46,47].

LTC was recalculated for the NW of diameter 229 nm as a reference to elucidate the role of each phonon scattering rate, as shown in figure 3. In bulk semiconductors, phonon-boundary scattering makes a significant contribution only below the temperature at

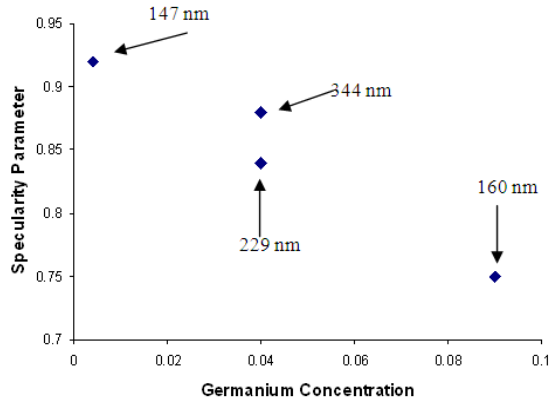


**Figure 2.** Variation in specularity parameter,  $P$ , as a function of Ge concentration for the four samples: 147, 344, 229 and 160 nm of  $Si_{1-x}Ge_x$  alloy NWs.

which the conductivity peak occurs, which is about  $T=0.05 \theta$  K [16,24]. In contrast, in NWs, boundary scattering has a very strong influence on LTC up to about 130 K, and it also controls the shape of the thermal conductivity curve, as is evident in figure 3 (solid red line). This result is in qualitative agreement with that of GaAs NWs [42], where the boundary effect has an influence up to around 100 K. At temperatures around the conductivity peak (in the bulk), mass disorder is important for lowering the LTC [16], as can be seen in figure 3, the LTC calculated for  $Si_{1-x}Ge_x$  alloy NWs without alloy scattering (solid black line) disappears at intermediate temperatures (between 170 and 260 K). While above 260 K, the curve suggests that U-processes are important. However, in bulk semiconductors for temperatures in the region of  $T=0.1 \theta$  K, the dominant phonon scattering mechanism is U-processes [33,53,54], but in this NW its influence becomes apparent above 260 K. These results suggest that alloy scattering plays a key role and is important in depressing and lowering the LTC with the coexistence of an anharmonicity contribution at intermediate and high temperatures, which is in good agreement with the experimental explanations at [21-23].

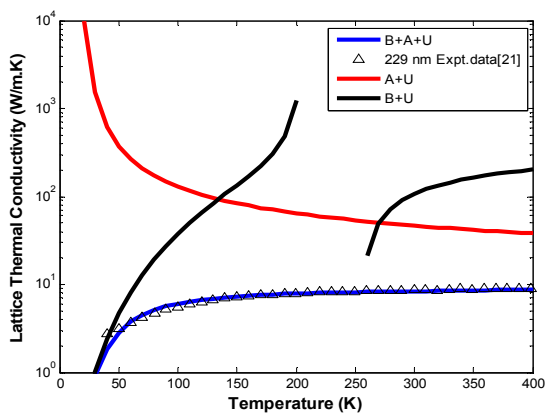


**Figure 3.** (Color online) Plot of temperature variation of the LTC of an  $Si_{1-x}Ge_x$  alloy NW of diameter 229 nm [21] as a reference. Lines represent the present theoretical results. Blue line: boundary(B), alloy(A) and Umkalpp(U) scattering rates. Red line: without B scattering rate. Black line: without A scattering rate.

To justifying the approach mentioned above, LTC was recalculated for an  $Si_{0.14}Ge_{0.86}$  alloy NW of diameter 161 nm [22], and compared with  $Si_{0.91}Ge_{0.09}$  alloy NW of diameter 160 nm [21]; the result is shown in figure 4A. For an  $Si_{0.14}Ge_{0.86}$  NW of diameter 161 nm,  $l$  is equal to 6.2 micrometers [22], and it was found that  $L_C = 50$  nm,  $\theta = 178$  K,  $P = 0.4$  and  $\gamma = 0.77$  for a best fit with the experimental data, and the decrease in  $L_C$  is due to high Ge concentration (86%) [22] which relates to the phonon-frequency dependence, as mentioned before.

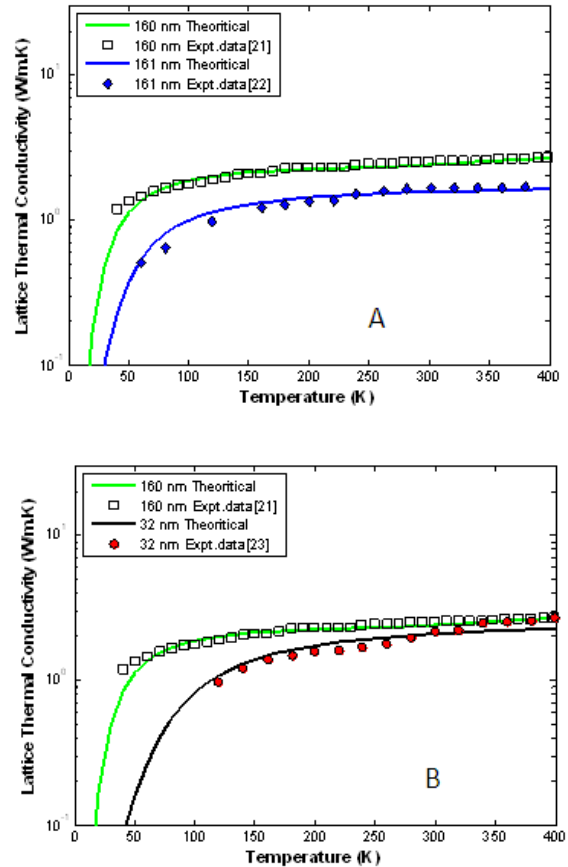


**Figure 4.** (Color online) LTC versus temperature for  $Si_{0.91}Ge_{0.09}$  alloy NW of diameter 160 nm for comparison with: (A)  $Si_{0.14}Ge_{0.86}$  alloy NW of diameter 161 nm, and (B)  $Si_{0.91}Ge_{0.09}$  alloy NW of diameter 32 nm. Solid lines are theoretical calculations. Experimental data are from [21-23].

As can be seen in figure 4A, the two NWs have (nearly) the same diameter, but the NW with a high alloy concentration has a lower LTC. This is due to the lower value of  $P$  and consequent high roughness as a result of the high alloy concentration (which relates to the mean free path as mentioned in figure 2), indicating that the surface effect at low temperatures, besides the alloy scattering at high temperatures (as elucidated in figure 3), will cause a reduction in the LTC. This result suggests that LTC is mainly depends on the alloy concentration, and the alloy effect causes a reduction in LTC for large diameters at low and high temperatures.

LTC was also recalculated for an  $Si_{0.91}Ge_{0.09}$  alloy NW of diameter 32 nm [23], which has the same Ge

concentration(0.09) as 160 nm at [21]; the result is shown in Fig.4B. For the NW of 32 nm, the values of  $\theta$  and  $\nu$  for Si and Ge were calculated via the same procedure that was used as in our previous work [44],  $l = 7$  micrometers [23] and  $L_C$  is limited by the sample diameter as 160 nm, it was found that  $\theta = 571$  K,  $P = 0.55$  and  $\gamma = 0.75$  for the best fit with the experimental data at [23]. Due to the small diameter, not only the surface effect but also the size effect will matter [47,50,55], and these causes a decrease in LTC below the room temperature. Above the room temperature, the alloy with an anharmonicity contribution will have the same effect as that of 160 nm. This result suggests that there is a size effect, in addition to the alloy effect, for a small diameter at low temperatures, while alloy scattering has the same effect as that of large diameters at high temperatures.

The role of the Gruneisen parameter,  $\gamma$ , can be clarified as follows: all analytical Gruneisen parameter values are based on approximations that rely upon a number of unjustified assumptions [54]. Therefore, this parameter is used as an adjustable parameter. The change in Gruneisen parameter is small (as shown in Table 2) in these NWs, indicating that the Gruneisen parameter is not size-dependent, unlike Si and Ge NWs [46,47]. Thus, anharmonicity is not as powerful as alloy scattering of these alloy NWs at high temperatures. This result suggests that alloy scattering is dominant not only at intermediate but also at high temperatures.

Finally, the role of the specularity parameter,  $P$ , can be clarified as shown in Fig.2, in that the dependency of  $P$  on the Ge concentration is due to the dominance of the alloy. For more elucidation of the effect of  $P$  on LTC, LTC is recalculated for a NW of diameter 229 nm, as a reference, for three values of  $P$  (0.55, 0.84, and 0.92) as shown in figure 5. Any change in the value of  $P$  will cause a large deviation from the experimental data. This result suggests that LTC mainly depends on the alloy concentration across the full range of temperatures.

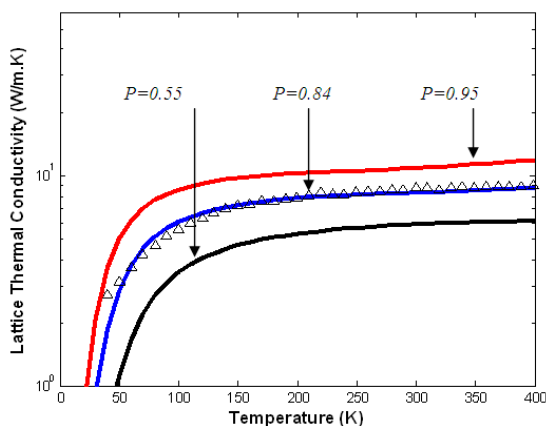


**Figure 5.** (Color online) Temperature dependence of LTC calculated for an  $\text{Si}_{1-x}\text{Ge}_x$  alloy NW of diameter 229 nm as a reference. Experimental data are from [21]. Solid lines are theoretical results for different values of the specularity parameter,  $P$ .

## 4. Conclusions

Acceptable calculations of LTC for temperatures between 20 and 400 K were obtained using Steigmeier and Abeles' model. The results were compared with those of experimental data in the literature. By adjusting the free parameters  $\theta$ ,  $P$ , and  $\gamma$  for the scattering rates considered in this work, good results were obtained. The results establish that alloy scattering is a powerful scattering mechanism in  $\text{Si}_{1-x}\text{Ge}_x$  alloy NWs. This alloy scattering is more dominant than U-processes at high temperatures, and LTC is mainly depends on the alloy concentration across the full range of temperatures. A weak diameter dependence for LTC was found, which is in reasonably good quantitative agreement with the experimental results. The anharmonicity and specularity parameters are not size-dependent, as compared to the case of Si and Ge NWs. Although alloy scattering is a major factor, phonon boundary scattering (surface and size effects) is also important in explaining the decrease in LTC of  $\text{Si}_{1-x}\text{Ge}_x$  alloy NWs at low temperatures.

## Acknowledgments

The author would like to express deep gratitude to Professor M. S. Omar, at the university of Salahaddin-Erbil, for his helpful guidance and encouragement throughout the period of this work; he has been a very valuable source of knowledge and insights. Also, the author would like to acknowledge the Faculty of Science and Science Education at the University of Sulaimani for their financial support.

## References

- [1] M. Pitkethly, Materials Today 7 (Supplement 1) (2004)20.
- [2] C. Lieber and Z. L.Wang, Mat. Res. Bull. 32 (2007) 99.
- [3] E.Sutter and P. Sutter, Nano Lett. 8 (2008) 411.
- [4] CRC Handbook of Thermoelectrics, edited by D. Rowe (CRC, Boca Raton, FL, 1995).
- [5] G. S. Nolas, J. Sharp and H. Goldsmid, Thermoelectrics: Basic Principles and New Materials Developments (Springer, New York, 2001).
- [6] Thermoelectrics Handbook: Macro to Nano, edited by D. Rowe (CRC, Boca Raton, 2006).
- [7] A. Majumdar, Science 303 (2004) 777.
- [8] M. S. Dresselhaus, G. Chen, M. Y. Tang, R. G. Yang, H. Lee, D. Z. Wang, Z. F. Ren, J. P. Fleurial and P. Gogna, Adv. Mater. 19 (2007) 1043.
- [9] G. Joshi, H. Lee, Y. Lan, X. Wang, G. Zhu, D. Wang, R. W. Gould, D. C. Cuff, M. Y. Tang and M. S. Dresselhaus, Nano Lett. 8 (2008) 4670.
- [10] D. Li, Y. Wu, P. Kim, L. Shi, P.Yang and A. Majumdar, Appl. Phys. Lett. 83 (2003) 2934.

- [11] A. I. Boukai, Y. Bunimovich, J. Tahir-Kheli, J. K. Yu, W. A. Goddard and J. R. Heath, *Nature* 451 (2008) 168.
- [12] X. Liu, R. Wang, Y. Jiang, Q. Zhang, X. Shan and X. H. Qiu, *Appl. Phys.* 108 (2010) 54310.
- [13] I. Hochbaum, R. Chen, R. Delgado, W. Liang, E. Garnett, M. Najarian, A. Majumdar and P. Yang, *Nature*, 451 (2008) 163.
- [14] C. Wood, *Rep. Prog. Phys.* 51 (1988) 459.
- [15] C. Bhandari and D. Rowe, *Contemp. Phys.* 21 (1980) 219.
- [16] G. A. Slack and M. S. Hussain, *J. Appl. Phys.* 70 (1991) 2694.
- [17] C. Vining, *J. Appl. Phys.* 69 (1991) 331.
- [18] C. Vining, W. Laskow, J. Hanson, V. Beck and P. D. Gorsuch, *Appl. Phys.* 69 (1991) 4333.
- [19] D. Rowe, L. Fu and S. G. Williams, *J. Appl. Phys.* 73 (1993) 4683.
- [20] J. Martinez, P. Provencio, S. Picraux, J. Sullivan and B. Swartzentruber, *Appl. Phys.* 110 (2011) 074317.
- [21] H. Kim, I. Kim, H. Choi and Woochul Kim, *Appl. Phys. Lett.* 96 (2010) 233106.
- [22] E. Lee, L. Yin, Y. Lee, J. Lee, S. Lee, J. Lee, S. Cha, D. Whang, G. Hwang, K. Hippalgaonkar, A. Majumdar, Ch. Yu, B. Choi, J. Min Kim and K. Kim, *Nano Lett.* 12 (2012) 2918.
- [23] L. Yin, E. Lee, J. Lee, D. Whang, B. Choi and Ch. Yu, *Appl. Phys. Lett.* 101 (2012) 043114.
- [24] P. G. Klemens, *Proc. Phys. Soc. LXVIII* 12-A (1955), P-1113.
- [25] A. Balandin and K. Wang, *Phys. Rev. B* 58 (1998) 1544.
- [26] D. Cahill, W. Ford, K. Goodson, G. Mahan, A. Majumdar, H. Maris, R. Merlin and S. Phillpot, *J. Appl. Phys.* 93 (2003) 793.
- [27] E. Steigmeier and B. Abeles, *Phys. Rev.* 136 (1964) A1149.
- [28] J. Callaway, *Phys. Rev.* 113 (1957) 1046.
- [29] E. Steigmeier and L. Kudman, *Phys. Rev.* 1M(1963) 508.
- [30] R. E. Peierls, *Ann. Phys. (Leipzig)* 3 (1929) 1055.
- [31] P. Carruthers, *Rev. of Mod. Phys.* 33 (1961) 9.
- [32] G. Slack and S. Galginaitis, *Phys. Rev.* 133 (1964) A253.
- [33] J. Zou, D. Kotchetkov, A. Balandina, D. Florescu and F. Pollak, *Appl. Phys.* 92 (2002) 2534.
- [34] Zh. Wang and N. Mingo, *Appl. Phys. Lett.* 97 (2010) 101903.
- [35] B. Abeles, *Phys. Rev.* 131 (1963) 1906.
- [36] H. G. Casimir, *Physica* 5 (1938) 495.
- [37] R. Berman, F. E. Simon and J. M. Ziman, *Proc. R. Soc. London, Ser. A* 220 (1953) 171.
- [38] J. M. Ziman, *Electrons and Phonons*, Oxford University Press, New York, 1967.
- [39] S. B. Soffer, *J. Appl. Phys.* 38 (1967) 1710.
- [40] J. Vandersande, *Phys. Rev. B* 15 (1977) 2355.
- [41] M. Kazan, G. Guisbiers, S. Pereira, M. Correia, A. Bruyant, S. Volz and P. Royer, *Appl. Phys.* 107 (2010) 083503.
- [42] S. Barman and G. Srivastava, *Phys. Rev. B* 73 (2006) 205308.
- [43] D. Morelli, J. Heremans, G. Slack, *Phys. Rev. B* 66 (2002) 195304.
- [44] S. M. Mamand, M.S. Omar, A.J. Muhammad, *Mater. Res. Bull.* 47 (2012) 1264.
- [45] A. Balandin, *Phys. Low-Dim. Structure*, 1/2 (2000) 1.
- [46] M. S. Omar and H. Taha, *Sadhana (Indian Academy of Sciences)*, 35 (2010) 177.
- [47] S. M. Mamand and M. S. Omar, *Adv. Mater. Res.* 832 (2014) 33.
- [48] Y. Ezzahria and K. Joulain, *J. Appl. Phys.* 112 (2012) 083515.
- [49] A. Balerna and S. Mobilio, *Phys. Rev. B* 34 (1986) 2293.
- [50] J. Zou and A. Balandin, *J. Appl. Phys.* 89 (2001) 2932.
- [51] J. Zou, *J. Appl. Phys.* 108 (2010) 034324.
- [52] L. Liu and X. Chen, *J. Appl. Phys.* 107 (2010) 033501.
- [53] G. A. Slack, *Phys. Rev.* 133 (1964) A253.
- [54] M. Asen-Palmer, K. Bartkowski, E. Gmelin, M. Cardona, A. Zhernov, A. Inyushkin, A. Taldenkov, V. Ozhogin, K. Itoh and E. Haller, *Phys. Rev. B* 56 (1997) 9431.
- [55] P. Martin, Z. Aksamija, E. Pop and U. Ravaioli, *Phys. Rev. Lett.* 102 (2009) 125503.